Understanding summertime H_2O_2 chemistry in North China Plain through observations and modelling studies

Can Ye[1], Pengfei Liu[2*], Chaoyang Xue[3*], Chenglong Zhang[2], Zhuobiao Ma[2], Chengtang Liu[2], Junfeng Liu[2], Keding Lu[4], Yujing Mu[2*], Yuanhang Zhang[4]

[1] School of Environmental Science and Engineering, Tiangong University, Tianjin 300387, China
[2] Research Center for Eco-Environmental Sciences, Chinese Academy of Sciences, Beijing 100085, China
[3] Max Planck Institute for Chemistry, Mainz 55128, Germany
[4] State Key Joint Laboratory of Environment Simulation and Pollution Control, College of Environmental Sciences and Engineering, Peking University, Beijing, 100871, China

Correspondence to: Pengfei Liu (pfliu@rcees.ac.cn) , Chaoyang Xue (ch.xue@mpic.de), Yujing Mu (yjmu@rcees.ac.cn)

Abstract.

Hydrogen peroxide (H_2O_2) is a key atmospheric oxidant, crucial for oxidation capacity and sulfate production. However, its chemistry remains understudied compared to ozone (O_3), limiting our understanding of photochemical pollution. In summer 2016, atmospheric peroxides and trace gases were measured at a rural site in the North China Plain. H_2O_2 was the dominant peroxide (0.62±0.80 ppb), constituting 69% of total peroxides. It exhibited diurnal variation similar to peroxyacetyl nitrate (PAN) and O_3, indicating photochemical production. The O_3/H_2O_2 ratio was higher on high-particle days, suggesting H_2O_2 uptake by particles reduces its concentration. A box model with default gas-phase chemistry overestimated H_2O_2 by a factor of 2.7, and including particle uptake of H_2O_2 (uptake coefficient: 6×10^{-4}) improved agreement with observations, although we note this value carries some uncertainty related to the assumed HO_2 uptake coefficient.

HO_2 recombination contributed 91% of H_2O_2 production, with a peak rate of 1 ppb h^{-1}. Major removal pathways included particle uptake (69%), dry deposition (25%), OH reaction (4%), and photolysis (2%). Relative incremental reactivity (RIR) analysis showed that reducing NO_x, $PM_{2.5}$, and alkanes increased H_2O_2, while reducing alkenes, aromatics, CO, and HONO decreased it, with alkenes having the strongest effect. H_2O_2/NO_z ratios (>0.15 in 82% of cases) indicated O_3 formation was in a transition and NO_x-sensitive regime, emphasizing the need for VOC and further NO_x reductions to mitigate both H_2O_2 and O_3 pollution. These findings improve our understanding of H_2O_2 chemistry and provide insights for mitigating photochemical pollution in rural North China.

1 Introduction

The atmospheric oxidation capacity is a critical determinant of atmospheric self-cleaning, influencing the residence time and persistence of pollutant gases. Quantifying this capacity is essential for elucidating the lifetimes of pollutants, the formation of aerosols, and their subsequent radiative forcing effects. Hydrogen peroxide (H_2O_2) serves as a significant atmospheric oxidant, primarily generated through the recombination of hydroperoxyl radicals (HO_2), which are themselves derived from reactions involving hydroxyl radicals (OH), volatile organic compounds (VOCs), and carbon monoxide (CO). Consequently, the formation of H_2O_2 is intrinsically linked to atmospheric oxidation capacity, with its concentration serving as a direct indicator of the intensity of this capacity. Furthermore, as H_2O_2 represents a terminal product in the ozone (O_3) formation chain reaction, its concentration can be utilized to assess the sensitivity of O_3 production to precursors (Sillman, 1995; Reeves and Penkett, 2003; Nunnermacker et al., 2008; He et al., 2010). Owing to its strong oxidative potential and high Henry's law constant, H_2O_2 readily dissolves in cloud droplets, where it oxidizes sulfur dioxide (SO_2) to form sulfuric acid (H_2SO_4), thereby contributing to sulfate aerosol formation and acid rain deposition (Calvert et al., 1985). Research indicated that H_2O_2-mediated oxidation of SO_2 in cloud water accounts for 60-80% of global SO_2 oxidation (Penkett et al., 1979; Calvert et al., 1985; Sofen et al., 2011). Additionally, recent studies have highlighted the significant role of particle-phase H_2O_2 oxidation in sulfate formation during winter (Ye et al., 2018; Ye et al., 2021b; Gao et al., 2024). Given its potent oxidative properties, H_2O_2 also poses substantial risks to human health and vegetation (Chen et al., 2010). Thus, a precise understanding of H_2O_2 chemistry is imperative for advancing knowledge of atmospheric oxidation processes and for diagnosing underlying secondary pollution formation mechanisms.

Atmospheric H_2O_2 concentrations are currently reported to range from 0.1 to 13 ppb (Balasubramanian and Husain, 1997; Walker et al., 2006; Ren et al., 2009; Guo et al., 2014; He et al., 2010; Qin et al., 2018; Fischer et al., 2015; Fischer et al., 2019; Ye et al., 2022; Allen et al., 2022; Zhang et al., 2018), with their spatial and temporal variability governed by a balance between production sources and removal pathways. H_2O_2 is generated through both primary and secondary sources. Primary sources of H_2O_2 include biomass burning, which can contribute substantially under specific conditions. For instance, Ye et al. (2022) reported elevated H_2O_2 concentrations during biomass combustion events, which promote secondary sulfate formation and thereby increase fine particulate matter ($PM_{2.5}$) concentrations. The dominant secondary source is the recombination of HO_2 radicals, a process enhanced during summer months due to increased solar radiation, which elevates HO_2 concentrations and consequently leads to higher H_2O_2 levels. However, under elevated nitrogen oxide (NOx) conditions, nitric oxide (NO) reacts competitively with HO_2, suppressing H_2O_2 formation and resulting in reduced atmospheric concentrations. Another secondary source involves the ozonolysis of alkenes, which produces Criegee intermediates that can decompose to form H_2O_2 (Becker et al., 1990). This pathway is particularly relevant during nighttime and potentially in winter, when photochemical activity is diminished (Lee et al., 2008b). For example, alkene ozonolysis was found to dominate wintertime H_2O_2 levels (>70%) (Qin et al., 2018), although the yields are generally low, often below 10%. Additionally, the release of H_2O_2 from the particle phase has been proposed as a potential source, though its contribution is considered negligible compared to gas-phase production. Recent studies, however, have highlighted that under polluted conditions, high concentrations of humic-like substances and transition metals can facilitate particle-phase H_2O_2 formation, which subsequently partitions into the gas phase, significantly enhancing gas-phase H_2O_2 levels (Ye et al., 2021b; Liu et al., 2021).

H_2O_2 can be removed by photolysis, which not only depletes H_2O_2 but also serves as a source of hydroperoxyl radicals (HOx). However, due to lower photolysis frequency, the contribution of H_2O_2 photolysis to atmospheric HOx production is generally much smaller compared to photolysis of O_3, nitrous acid (HONO), and formaldehyde (HCHO). Notably, particle-phase H_2O_2 photolysis has been identified as a critical source of free radicals within aerosols, accelerating aerosol aging and promoting the formation of secondary pollutants. Rao et al. (2023) further emphasized a significantly accelerated rate for air-water interface H_2O_2 photolysis, underscoring its importance as a source of particle-phase OH. Dry deposition is another key removal mechanism, leading to a vertical gradient in H_2O_2 concentrations, with peak levels observed at approximately 2 km above the surface (Watanabe et al., 2016; Klippel et al., 2011). Due to its high solubility, wet deposition through rainwater scavenging also effectively removes H_2O_2 from the atmosphere. Moreover, laboratory and field studies have demonstrated that heterogeneous uptake by particles can significantly contribute to H_2O_2 removal under polluted conditions. Qin et al. (2022) reported a maximum uptake coefficient of 2.49×10^{-3} for H_2O_2 by ambient particles, with the uptake coefficient influenced by the concentration of transition metals within the particles.

In addition to H_2O_2, the atmosphere contains a variety of organic peroxides, such as methyl hydroperoxide (CH_3OOH), formed through reactions between HO_2 and organic peroxy (RO_2) radicals. While H_2O_2 is the most abundant peroxide in the atmosphere, organic peroxides are recognized as a significant component of secondary organic aerosol (SOA), contributing to aerosol composition and properties. However, due to analytical challenges associated with measuring organic peroxides, most studies on atmospheric peroxides have only focused on H_2O_2 (Zhang et al., 2012).

Photochemical pollution has emerged as a critical air quality issue in China, impacting both urban and rural regions. H_2O_2 and O_3 are key products of photochemical pollution, and elucidating their chemical behavior is essential for developing effective strategies to mitigate photochemical pollution. However, compared to the extensive research on O_3, studies on H_2O_2 remain limited due to the technical challenges and complexities associated with its measurement. In recent years, O_3 concentrations in the North China Plain have exhibited a significant upward trend (Li et al., 2019; Wang et al., 2020; Lu et al., 2020), yet the characteristics of H_2O_2 in this region remain poorly understood. Furthermore, the implementation of national emission reduction policies has led to a substantial decline in NOx, while VOCs persist at elevated levels (Liu et al., 2023). This shift toward low NOx and high VOCs conditions is more conducive to H_2O_2 formation. Although photochemical pollution is traditionally considered as an urban phenomenon, recent studies have highlighted its increasing prevalence in rural areas, where pollution levels are gradually approaching those observed in urban areas (Ma et al., 2016). Rural regions typically exhibit lower NOx concentrations than urban areas, creating conditions more favorable for H_2O_2 production. Despite this, research on H_2O_2 in rural areas of the heavily polluted North China Plain remains scarce. Consequently, there is an urgent need to investigate H_2O_2 chemistry in rural environments to inform targeted control strategies for photochemical pollution.

This study is based on a field campaign conducted in a rural area of the North China Plain, during which a comprehensive suite of gaseous (including H_2O_2), particulate matter, and meteorological parameters, were measured. Here we investigate the temporal variations of H_2O_2, and its relationships with other oxidants (e.g., O_3 and peroxyacetyl nitrate, PAN), and preliminarily estimate organic peroxide concentrations. A zero-dimensional box model was employed to examine the influence of particles on the H_2O_2 budget and the sensitivity of H_2O_2 production to various chemical species. Finally, we explore the potential of H_2O_2 as an indicator for determining O_3 sensitivity and discuss the control strategy for alleviating photochemical pollution.

2 Experiments

2.1 Measurement site

The observational experiment was conducted at the Station of Rural Environment, Research Center for Eco-Environmental Sciences (SRE-RCEES, 38°42′N, 115°15′E), located in Dongbaituo Village, Wangdu County, Hebei Province. Situated approximately 180 km southwest of Beijing, the station is surrounded primarily by farmland with no nearby industrial facilities, making it an ideal site for studying typical rural atmospheric conditions. This location has historically served as a key site for numerous large-scale observational campaigns (Tan et al., 2017; Peng et al., 2021). The experiment took place from 6 July 2016 to 12 August 2016, with the primary objective of investigating the underlying causes of photochemical pollution in the rural North China Plain.

2.2 H_2O_2 measurements

H_2O_2 concentrations were measured using the AL-2021 H_2O_2 monitor (Aero-Laser) (Lazrus et al., 1986). The instrument operates on the following principle: gas-phase peroxides in ambient air are collected by buffered solution in a glass stripping coil. The trapped peroxides then react with p-hydroxyphenyl acetic acid (POPHA) under the catalysis of peroxidase, producing a fluorescent dimer. This dimer exhibits maximal light absorption at a characteristic wavelength of 320 nm and emits fluorescence with a central wavelength of 400 nm. By continuously monitoring the intensity of this fluorescence signal, the instrument enables online quantitative detection of atmospheric peroxides. To differentiate between H_2O_2 and organic peroxides, a dual-channel measurement approach was employed. Channel A measures the total peroxide content, while Channel B incorporates catalase into the absorbent solution to selectively decompose H_2O_2, thereby measuring only organic peroxides. The H_2O_2 concentration is determined by the difference in signals between the two channels. Although Channel B provides an approximation of organic peroxides, it is important to note that the percentage of organic peroxides reported in this study represents a lower limit, as the collection efficiency of the stripping coil technique varies significantly among different organic peroxide species. While H_2O_2 is efficiently trapped due to its high solubility (Henry's law constant: ~10^5 M atm^{-1}), many organic peroxides such as methyl hydroperoxide (MHP) have substantially lower solubilities (Henry's law constant: 3×10^2 M atm^{-1}), resulting in lower collection efficiencies. Additionally, the catalase used to differentiate between H_2O_2 and organic peroxides may not completely discriminate between certain hydroperoxide species, further contributing to uncertainty in organic peroxide quantification. The detection limit of the H_2O_2 measurement instrument is 50 ppt, with an uncertainty of 10%. To ensure the stability of the instrument's operation, regular calibrations are performed at fixed intervals. In several previous field experiments (Ye et al., 2018; Ye et al., 2021b; Ye et al., 2021a; Liu et al., 2021), this instrument has been successfully utilized to measure atmospheric H_2O_2, demonstrating high reliability and consistent operational stability.

2.3 Other species

NOx, O_3, SO_2, $PM_{2.5}$, CO, and total reactive nitrogen (NOy) were measured using commercial instruments from Thermo Electron. Volatile organic compounds (VOCs) were quantified by gas chromatography with a flame ionization detector (GC-FID), while nitrous acid (HONO) was measured using a long-path absorption photometer (LOPAP) from QUMA. The aerosol surface area density was calculated by combining data from a scanning mobility particle sizer (SMPS) and an aerodynamic particle sizer (APS). PAN was analyzed using gas chromatography with electron capture detection (GC-ECD). Gas-phase meteorological data were collected using a portable meteorological station (Model WXT520, Vaisala, Finland). The photolysis rate constant of NO_2 ($j(NO_2)$) was measured directly, and other photolysis rate constants were derived using the Tropospheric Ultraviolet and Visible (TUV) radiation model, scaled based on $j(NO_2)$ measurements. Detailed information on the experimental instruments is provided in Table S1.

2.4 Box model descriptions

A zero-dimensional box model based on the RACM2-LIM1 mechanism was employed to investigate the sources and removal mechanisms of H_2O_2. This model is widely recognized for its ability to accurately model HOx radicals (Tan et al., 2017; Ma et al., 2022). Given that the HO_2 is a critical precursor for H_2O_2 formation, the model's strong performance in simulating free radicals provides confidence in its ability to reliably simulate H_2O_2 concentrations. The model was constrained using input parameters including photolysis rate constants ($j(NO_2)$, $j(O^1D)$, j(HONO), $j(H_2O_2)$, j(HCHO)), VOCs, NO, NO_2, O_3, HONO, methane (CH_4), CO, and meteorological data (temperature, relative humidity, and pressure). VOCs were categorized into different reactivity-based groups according to their reaction rates with OH, as detailed in Table S2. The dry deposition rate constant for H_2O_2 was set to 3×10^{-5} s^{-1}, and boundary layer heights were derived from the hybrid single-particle Lagrangian integrated trajectory (HYSPLIT) model.

The simulation focused on the period from 24 July to 3 August, selected for its stable meteorological conditions, characterized by low wind speeds and predominantly static weather. During this period, the observed trends in H_2O_2 concentrations exhibited consistent patterns, suggesting that local photochemical processes were the primary source of H_2O_2. This makes the selected timeframe ideal for exploring H_2O_2 sources using the box model. Additionally, elevated $PM_{2.5}$ concentrations during this period provided an opportunity to investigate the potential influence of particle uptake on H_2O_2 removal. The rate coefficient of H_2O_2 uptake by particles was parameterized as equation 1:

$$k=0.25\times c\times\gamma\times S_a \quad \text{Eq. 1}$$

Here c is mean molecular speed of H_2O_2, γ is the H_2O_2 uptake coefficient, and S_a is aerosol surface area density.

To assess the contributions of different precursors to H_2O_2 production, Relative Incremental Reactivity (RIR) analysis was conducted. RIR was calculated using the following equation:

$$\mathrm{RIR}(X)=\frac{\frac{\Delta H_2O_2(X)}{H_2O_2}}{\frac{\Delta C(X)}{C(X)}} \quad \text{Eq. 2}$$

In Eq.2, X represents the primary pollutants that may influence H_2O_2 concentrations. H_2O_2 represents modelled H_2O_2 in the base case. $\Delta C(X)/C(X)$ represents the relative change of primary pollutants. $\Delta H_2O_2(X)/H_2O_2$ represents the relative change of modelled H_2O_2 concentrations induced by the reduction of X. Considering the variations in simulated radical concentrations and the deviations in the RIR, a 20% reduction scenario was selected for further analysis. This approach allowed for the quantification of the sensitivity of H_2O_2 production to variations in precursor concentrations, providing insights into the key drivers of H_2O_2 formation in the rural North China Plain.

3 Results and discussion

3.1 Time series overview

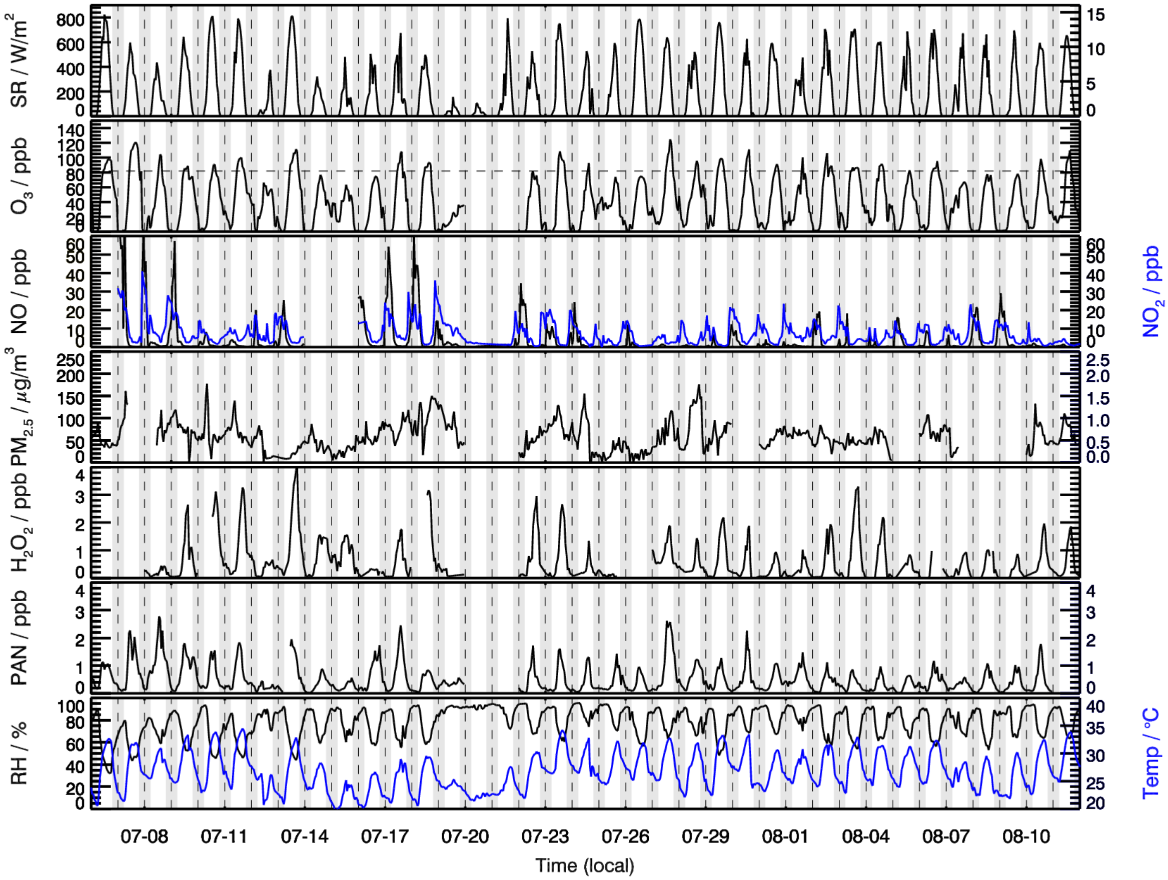

Figure 1. Measurements of H_2O_2, other related chemical species and meteorological parameters at SRE-RCEES site during the observation period.

Throughout the observation period, meteorological conditions were characterized by high temperature and relative humidity. High temperature generally increased the rate constants of photochemical reactions, while abundant water vapor enhanced the recombination rate of HO_2 and the reaction rate between $O(^1D)$ and water vapor (H_2O). The maximum O_3 concentration reached 120 ppb, with the maximum daily 8-hour average (MDA8) frequently exceeding the National Ambient Air Quality Standard (NAAQS) Class-II standard of 82 ppb (25 ℃, 1013 *kPa*). High O_3 pollution events often coincided with elevated H_2O_2 concentrations (>2 ppb), suggesting that O_3 production at this site may be sensitive to NOx. This hypothesis will be further investigated using the H_2O_2/NOz and O_3/NOz in Section 3.6 on O_3 sensitivity. NOx concentrations peaked in the morning, driven by factors such as traffic emissions and lower boundary layer height. Daytime NO concentrations were generally below 1 ppb, while daily peak H_2O_2 concentrations exhibited significant day-to-day variability, ranging from approximately 0.2 ppb to 4 ppb. Higher H_2O_2 concentrations were observed during periods of intense solar radiation, indicating that local photochemical reactions play a significant role in H_2O_2 production. Notably, elevated H_2O_2 levels were only observed when NO concentrations were low, consistent with the known mechanism of H_2O_2 formation under low NOx conditions.

The average H_2O_2 concentration during the whole observation period was 0.62±0.80 ppb, significantly higher than wintertime concentrations (0.19 ppb) at the same site (Ye et al., 2021b), as summer conditions with high solar radiation intensity and relative humidity are more conducive to H_2O_2 production. This average concentration also exceeded summer H_2O_2 levels reported in urban areas, such as Beijing (0.27 pb) (Qin et al., 2018) and Hong Kong (0.32 ppb) (Guo et al., 2014), likely due to lower NOx levels at the rural site, which favor H_2O_2 formation. Compared to H_2O_2 concentrations reported at rural sites in other countries, the levels observed in this study were lower than that in Kinterbish (Watkins et al., 1995), Whiteface Mountain (1.61 ppb) (Balasubramanian and Husain, 1997). It is worth mentioning that, an average H_2O_2 concentration of 0.51±0.90 ppb was reported at the same site in summer 2014 (Wang et al., 2016), lower than the current study's findings, reflecting a potential increasing trend in H_2O_2 concentrations over time. In addition, multi-year measurements at the summit of Mount Tai revealed an increasing trend of H_2O_2 concentrations in cloud water from 2014 to 2018 (Li et al., 2020), indirectly indicating rising gas-phase H_2O_2 levels in the North China Plain. The significant reduction in NOx emissions in the North China Plain over recent years, while VOC levels remained relatively high or decreased less sharply, has likely shifted the atmospheric chemistry towards conditions more favorable for HO_2 recombination, potentially contributing to the observed increasing trend in H_2O_2 concentrations. This aligns with the known sensitivity of H_2O_2 formation to NOx levels.

Elevated H_2O_2 concentrations and high relative humidity in rural areas facilitate the oxidation of SO_2 by H_2O_2 in both aerosol water and cloud water, contributing to sulfate formation and increased $PM_{2.5}$ levels. During the observation period, the average $PM_{2.5}$ concentration reached 57 μg m^{-3}, and the co-occurrence of $PM_{2.5}$ and O_3 pollution was frequently observed. This dual pollution phenomenon suggests that high concentrations of oxidants may play a significant role in driving secondary aerosol formation. PAN, another key secondary oxidant measured in this study, reached a maximum concentration of 2.9 ppb. Similar to H_2O_2 and O_3, PAN is a product of photochemical pollution, and its temporal trends closely mirrored those of H_2O_2 and O_3. These trends will be analyzed in detail in the section 3.2. As strong oxidizing agents, H_2O_2, O_3 and PAN are proven to be damaging to vegetation and human health. Given the high concentrations of these oxidants observed in this study, photochemical pollution in rural areas poses serious risks to agricultural productivity and human health.

3.2 Diurnal patterns of three photochemical oxidants

The average diurnal trends of H_2O_2, PAN, and O_3 exhibited pronounced daily variations, with concentrations peaking during the daytime and declining at night (Figure 2). These trends closely followed solar radiation patterns, highlighting the significant contribution of photochemical reactions to their formation. In addition, the pronounced daily variations also indicated the presence of abundant precursors in the region facilitating the production of H_2O_2, PAN, and O_3. In the early morning, as solar radiation intensified, the photolysis of HONO initiated daytime photochemical reactions (R0), generating peroxyl radicals (R1). These radicals reacted with NO to produce O_3 (R2-R5); HO_2 recombination underwent bimolecular recombination to produce H_2O_2 (R6); peroxyacetyl radicals (PA) reacted with NO_2 to form PAN (R7). These processes led to a rapid increase in the concentrations of all three oxidants, with peak concentrations reaching 1.8 ppb, 1.2 ppb, and 84 ppb for H_2O_2, PAN, and O_3, respectively.

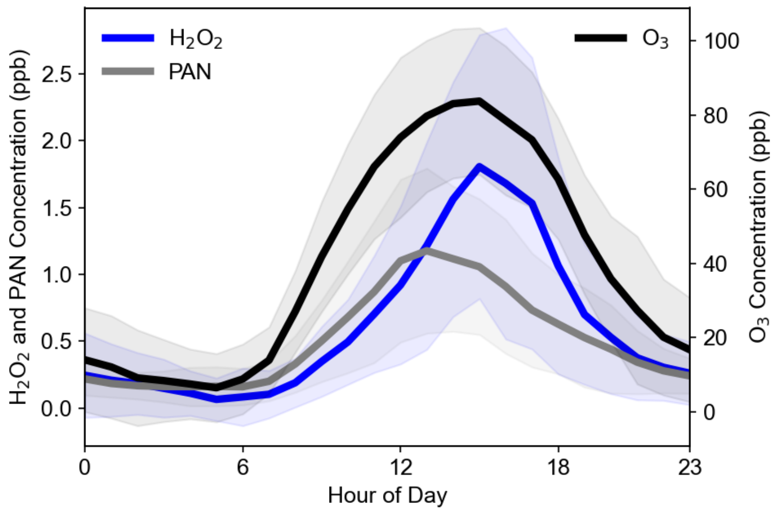

Figure 2. Average diurnal cycles of H_2O_2, PAN, and O_3 observed throughout the entire campaign period at the SRE-RCEES site.

Despite sharing similar photochemical formation pathways, the peak times of the three oxidants differed due to variations in their production and removal rates. PAN concentrations peaked around noon, approximately 2–3 hours earlier than H_2O_2 and O_3, a phenomenon also observed in previous studies (Lee et al., 2008a). This earlier peak for PAN can be attributed to its higher thermal decomposition rate at midday. In contrast, the peaks for H_2O_2 and O_3 both occurred around 16:00. Notably, in urban areas, H_2O_2 peaks often lag behind O_3 peaks. For example, observations at the urban Tai'an site in the North China Plain revealed that H_2O_2 peaks occurred approximately 2 hours after O_3 peaks (Ye et al., 2021a). This delay can be explained by HO_2 chemistry under varying NOx conditions. Under high NOx condition, HO_2 primarily reacts with NO (reaction rate constant: 8.9×10^{-12} cm^3 $molecule^{-1}$ s^{-1} at 298 *K*), whereas under low NOx condition, HO_2 undergoes bimolecular recombination to form H_2O_2 (reaction rate constant: 1.5×10^{-12} cm^3 $molecule^{-1}$ s^{-1} at 298 *K*). In urban settings, H_2O_2 peaks only occur when NO concentrations drop to around 100 ppt, allowing HO_2 recombination to dominate, thus delaying the H_2O_2 peak relative to O_3. However, at this rural site, daytime NO concentrations were consistently low, resulting in simultaneous peaks for O_3 and H_2O_2.

$HONO + h\upsilon \rightarrow OH + NO$ R0

$VOCs + OH \rightarrow RO_2 + H_2O$ R1

$RO_2 + NO \rightarrow HO_2 + RO_2 + OVOC$ R2

$HO_2 + NO \rightarrow NO_2 + OH$ R3

$NO_2 + h\upsilon \rightarrow NO + O(^3P)$ R4

$O(^3P) + O_2 \rightarrow O_3$ R5

$HO_2 + HO_2 + M \rightarrow H_2O_2 + H_2O + M$ R6

$CH_3C(O)OO + NO_2 + M \rightarrow CH_3C(O)OONO_2(PAN) + H_2O + M$ R7

Following their peaks, the concentrations of all three oxidants declined rapidly. For H_2O_2, this decrease was primarily driven by dry deposition and, in the evening, enhanced uptake by liquid aerosols formed as relative humidity increased. O_3 concentrations dropped due to a combination of dry deposition and NO titration, while PAN levels decreased mainly through thermal decomposition. At night, the absence of photochemical reactions caused all three oxidants to maintain low concentrations.

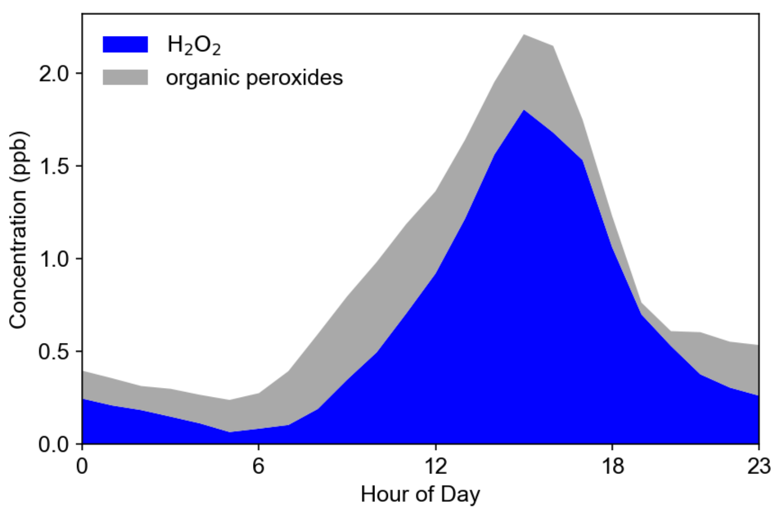

Figure 3. Average diurnal cycles of H_2O_2 and organic peroxides (ROOH) observed throughout the entire campaign period at the SRE-RCEES site.

Figure 3 illustrates the average diurnal trends of ROOH and H_2O_2. The trends of total peroxides closely align with those of H_2O_2, indicating similar production and removal mechanisms. H_2O_2 accounts for 69% of the total peroxides on average, while ROOH (0.28 ppb) constitute 31%. This demonstrates that peroxides in rural areas are predominantly dominated by H_2O_2, consistent with the findings of Wang et al. (2016) at this site. However, it is important to note that the percentage of ROOH reported in this study represents a lower limit, as not all ROOH are fully captured by the measurement technique. In contrast, Liang et al. (2013) reported that ROOH accounted for 80% of total peroxides in urban areas such as Beijing. The difference in organic peroxide proportions between Beijing and Wangdu can likely be attributed to variations in chemical conditions, such as differences in VOC compositions, which influence the types and abundances of peroxyl radicals formed. The diurnal variation in the relative contributions of H_2O_2 and ROOH to total peroxides, reflects their distinct production and loss mechanisms. H_2O_2 dominates (over 90%) around 19:00 due to strong photochemical production via HO_2 recombination during the day, while its contribution drops to ~25% by 05:00 due to nighttime losses (e.g., heterogeneous uptake and dry deposition) without replenishment. In contrast, ROOH contribute more significantly in the early morning, likely due to slower loss rates compared to H_2O_2. ROOH such as CH_3OOH (methyl hydroperoxide) have much lower dry deposition rates—approximately 30 times lower than that of H_2O_2-leading to less nighttime loss and a higher relative contribution to total peroxides during early morning hours. The minimum in ROOH concentration observed around 19:00 represents a transitional point. By this time, daytime photochemical production has largely ceased due to diminishing solar radiation, leading to a decline from its afternoon peak as removal processes continue. The subsequent increase in ROOH concentration after 19:00, which makes 19:00 a local minimum, may be attributed to nighttime chemical production primarily through (a) the ozonolysis of alkenes (O_3 + alkenes → … → RO_2 → ROOH), and (b) NO_3 radical-initiated oxidation of VOCs (NO_2 + O_3 → NO_3; NO_3 + VOCs → … → RO_2 → ROOH). These processes become major sources of RO_2 (and subsequently ROOH) during the night. In contrast, H_2O_2 typically continues to decrease throughout the night. Although ozonolysis can also be a source H_2O_2, H_2O_2 generally has a higher dry deposition velocity than many ROOH species, leading to more efficient net removal overnight. These differences highlight the distinct photochemical dynamics and loss mechanisms of H_2O_2 compared to ROOH, influenced by diurnal variations in radiation, precursor concentrations, and meteorological conditions.

3.3 Correlations between different atmospheric oxidants

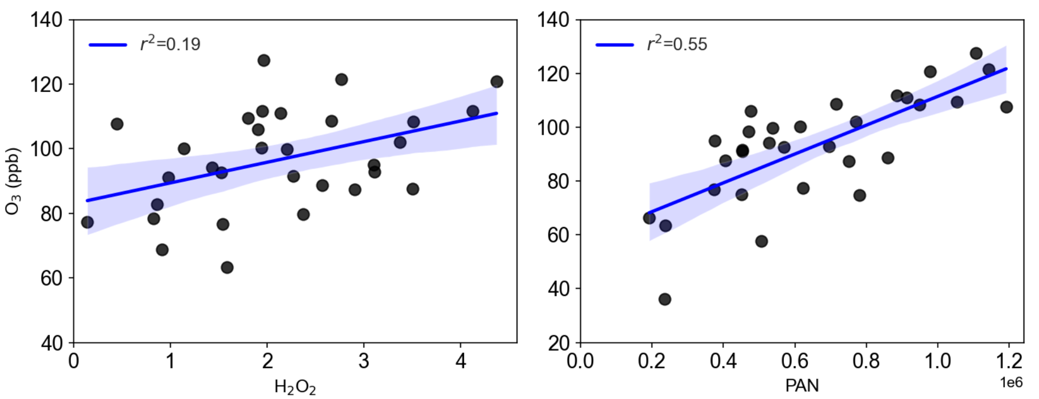

Figure 4. Correlations of O_3 daily maximum with H_2O_2 and PAN daily maximum

The formation of H_2O_2, O_3, and PAN is closely linked to VOCs, NOx, and solar radiation. Consequently, their concentrations are typically elevated and well-correlated during photochemical pollution episodes. Here, we investigate the relationships among these oxidants. Figure 4 illustrates the correlations between the daily maximum concentrations of H_2O_2, O_3, and PAN. A good correlation (r^2 = 0.55) was observed between PAN and O_3, consistent with previous studies (Lee et al., 2008a; Zhang et al., 2014; Xu et al., 2021; Sun et al., 2020). In contrast, the correlation between H_2O_2 and O_3 was weak (r^2 = 0.19). Prior research has shown positive correlations between H_2O_2 and O_3 during photochemical pollution due to their shared dependence on VOC and NOx photochemistry (Hua et al., 2008; Takami et al., 2003; Ye et al., 2021a; Guo et al., 2022), while negative correlations have been reported in clean marine boundary layer where O_3 photolysis dominates radical production (Ayers et al., 1992). The lack of a positive correlation between O_3 and H_2O_2 in this rural polluted environment may indicate additional factors influencing H_2O_2 concentrations. Notably, heterogeneous uptake by particles has been shown to affect H_2O_2 levels (De Reus et al., 2005; Qin et al., 2018), and given the relatively high $PM_{2.5}$ concentrations during the observation period, we hypothesize that heterogeneous loss reduces gas-phase H_2O_2, weakening its correlation with O_3. Additionally, aqueous-phase reactions in aerosol water or cloud droplets, facilitated by high relative humidity during the campaign, could further reduce gas-phase H_2O_2 without affecting O_3, contributing to the decoupling of their peak values. While the focus on daytime maxima limits the direct relevance of nighttime chemistry, processes such as alkene ozonolysis or nocturnal deposition could influence background H_2O_2 levels, indirectly affecting daytime peaks.

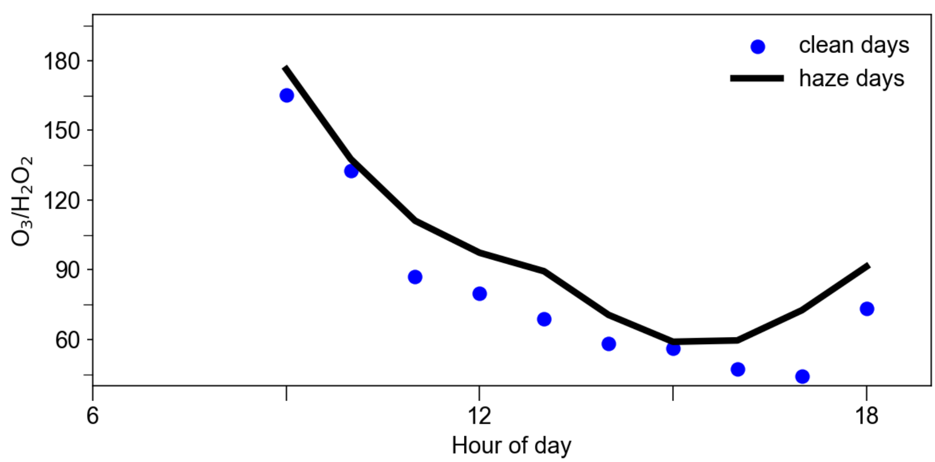

Figure 5. Average O_3/H_2O_2 from 9:00 to 18:00 on clean (daily average $PM_{2.5}$<50 μg m^{-3}) and polluted days (daily average $PM_{2.5}$≥ 50 μg m^{-3}).

To test this hypothesis, we analyzed the O_3/H_2O_2 ratio on polluted (daily average $PM_{2.5}$<50 μg m^{-3}) and clean days (daily average $PM_{2.5}$≥ 50 μg m^{-3}). While O_3 and H_2O_2 share similar photochemical formation pathways, O_3 is less affected by particle uptake. O_3 lifetime was estimated to be 13 days with respect to heterogeneous uptake for dust mass concentrations of 1000 μg m^{-3}, highlighting the minor role of particle uptake on O_3 removal (Tang et al., 2017). If the O_3/H_2O_2 ratio remains stable across polluted and clean conditions, heterogeneous uptake likely has minimal impact on H_2O_2. However, if the ratio is higher during polluted periods, it is possible that $PM_{2.5}$ may scavenge H_2O_2 by heterogeneous uptake. As shown in Figure 5, the O_3/H_2O_2 ratio during peak photochemical hours (9:00–18:00) was markedly higher on polluted days compared to clean days, supporting the hypothesis that heterogeneous uptake by $PM_{2.5}$ significantly reduces H_2O_2 concentrations. It is important to note that this method provides only a preliminary assessment, as uncertainties exist due to differences in the dependence of H_2O_2 and O_3 on peroxyl radical concentrations and their respective responses to radiation intensity. In addition, differences in photochemical regimes, potentially driven by varying VOC/NOx ratios between clean and polluted days, could also influence the O_3/H_2O_2 relationship independently of particle uptake effects. In the following section, we further examine the impact of $PM_{2.5}$ on H_2O_2 budget using a box model.

3.4 Investigation on H_2O_2 budget

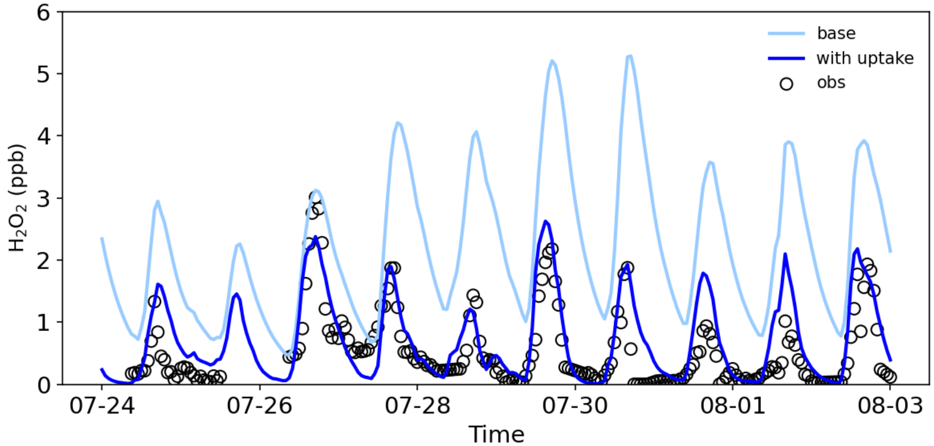

Figure 6. Observed and modelled H_2O_2 concentrations from 24 July to 3 August.

To better understand the sources and removal mechanisms of H_2O_2, we employed a box model to simulate its concentrations. As shown in Figure 6, base simulations using the model's default H_2O_2 source and removal mechanisms overestimated H_2O_2 concentrations compared to observations, with a simulated-to-measured ratio of 2.7. This discrepancy suggests an unaccounted removal pathway, consistent with our earlier hypothesis of H_2O_2 removal by particle uptake. When a parameterized uptake mechanism with an uptake coefficient of 6×10^{-4} was incorporated into the box model, the simulated H_2O_2 concentrations and trends aligned well with observed values (Fig. 6), confirming the significant role of particle uptake in H_2O_2 removal in rural areas. This uptake coefficient is comparable with the value (5×10^{-4}) estimated during a dense Saharan dust event (De Reus et al., 2005), and lower than 1×10^{-3} reported by Wang et al. (2016), which may be likely due to differences in particulate matter composition. Sensitivity tests indicated that an uptake coefficient of 1×10^{-3} resulted in underestimation (Figure.S1), supporting 6×10^{-4} as the optimal value for our study. This coefficient falls within the range (10^{-4}-10^{-3}) determined in laboratory studies for H_2O_2 uptake on ambient particles collected on filters or artificial particles

(Pradhan et al., 2010; Romanias et al., 2012; Qin et al., 2022). We believe this value represents a reasonable estimate for the conditions at our sampling site, though we acknowledge that a more dynamic treatment of heterogeneous processes that accounts for variations in aerosol composition, phase state, and ambient RH would be valuable in future studies.

It should be mentioned that previous studies have demonstrated that considering HO_2 by particles can partially explain the discrepancy between observed and modeled HO_2 concentrations under low NOx conditions (Kanaya et al., 2007a; Kanaya et al., 2007b; Whalley et al., 2010; Ma et al., 2022), as well as the phenomenon of increasing O_3 concentrations with decreasing particulate matter levels (Li et al., 2019). Since HO_2 is a precursor to H_2O_2, its uptake by particles naturally reduces H_2O_2 concentrations. However, laboratory-measured HO_2 uptake coefficients exhibit significant variability, ranging from 10^{-5} to 0.82, and are strongly influenced by the composition of particulate matter (Thornton et al., 2008; Taketani et al., 2012; George et al., 2013; Lakey et al., 2015). Through analysis of measured radical budget and related parameters, Tan et al. (2020) showed that the HO_2 uptake was not important in the North China Plain in 2014, with an uptake coefficient of 0.08. Given that our observational experiments were conducted at the same site with similar particulate matter composition, we also assumed an HO_2 uptake coefficient of 0.08 to investigate its impact on the H_2O_2 budget. Under this assumption, we found that an H_2O_2 uptake coefficient of 4.5×10^{-4} resulted in a good agreement between modeled and observed H_2O_2 concentrations (Figure S1). The results indicate that considering HO_2 uptake reduces the H_2O_2 uptake coefficient by 25%. Therefore, uncertainties in the HO_2 uptake coefficient significantly affect the accurate simulation of H_2O_2 concentrations and the estimation of the H_2O_2 uptake coefficient. A more precise parameterization scheme for HO_2 uptake is critical for models to accurately assess the global distribution of H_2O_2 concentrations and their environmental impacts.

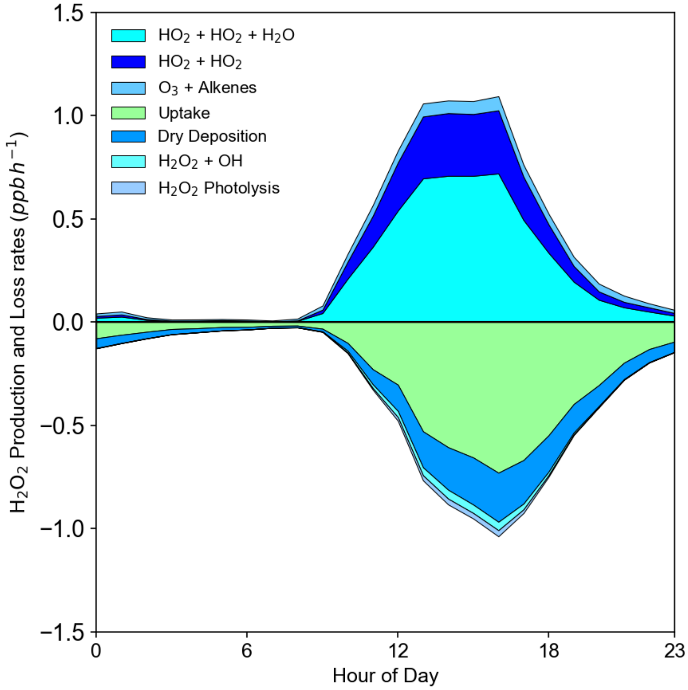

Figure 7. Modelled H_2O_2 sources and sinks.

Figure 7 depicts the H_2O_2 production rates and removal rates by different pathways. The percentage contribution of different pathways is shown in Figure S2. HO_2 bimolecular recombination was identified as the dominant H_2O_2 production pathway, contributing to 80% H_2O_2 production with a maximum yield of 1.0 ppb h^{-1} at noon. This highlighted rapid photochemical production as the primary driver of H_2O_2 pollution in the rural site. In contrast, the reaction of O_3 with alkenes accounted for 9% H_2O_2 production (Figure S2), with a maximum yield of 0.07 ppb h^{-1}, primarily from O_3+OLI reactions. This mechanism was found to be significant during winter pollution due to high alkenes and NO concentrations inhibiting HO_2 recombination (Qin et al., 2018). Heterogeneous uptake dominated H_2O_2 removal, accounting for 69% with a maximum removal rate of 0.7 ppb h^{-1}, underscoring its importance during summer pollution periods. Dry deposition, photolysis, and reaction with OH radicals contributed to 25%, 2%, and 4% H_2O_2 loss, respectively. These findings provide a comprehensive understanding of H_2O_2 sources and sinks in rural environments, emphasizing the critical role of particle uptake in H_2O_2 budget.

3.5 Precursors control to mitigate H_2O_2 pollution

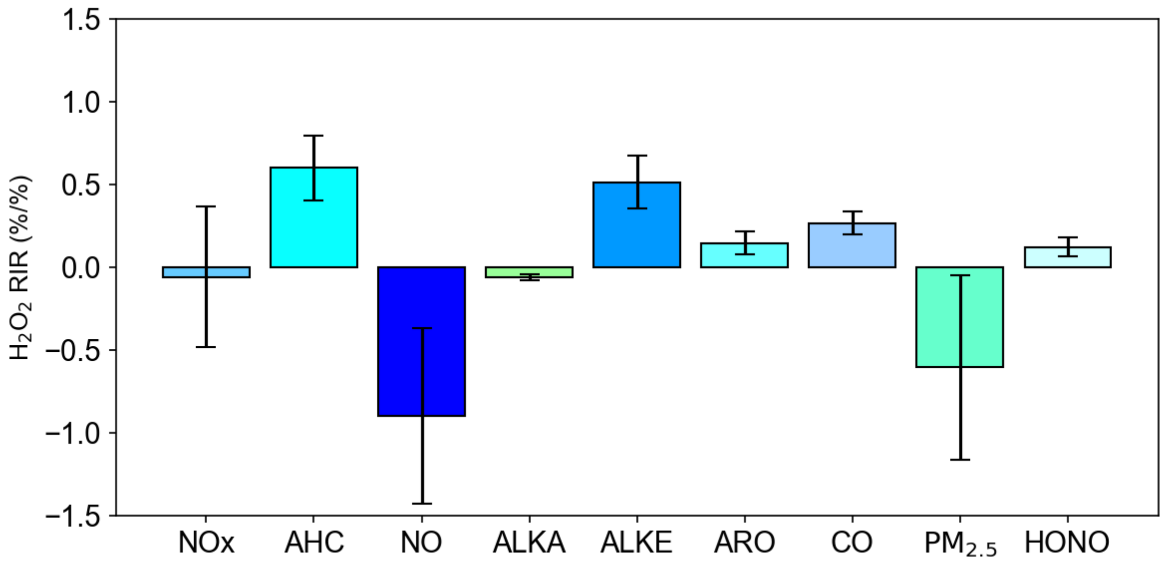

Figure 8. Sensitivity of H_2O_2 production to different chemical species.

It is evident that photochemical pollution in rural areas is associated with elevated concentrations of H_2O_2, necessitating urgent measures to mitigate H_2O_2 pollution by regulating its precursor compounds. Given the diversity of precursors involved in H_2O_2 formation, a critical objective is to quantify the relative contribution of each precursor to H_2O_2 pollution to establish prioritized control strategies. In this study, the RIR method was employed to identify the most effective pollutants for H_2O_2 control (Figure 8). Here it should be noted that the RIR analysis was performed using the adjusted model with H_2O_2 uptake coefficient of 6×10^{-4} that showed good agreement with observations. The results demonstrate that reducing NO concentrations leads to an increase in H_2O_2 levels, as the reaction between NO and HO_2 inhibits H_2O_2 production. However, under realistic conditions, a decrease in NO also results in reduced NO_2 levels. Since the NO_2 heterogeneous reaction is a significant source of HONO, which serves as a key precursor for OH influencing H_2O_2 formation, a decline in NO_2 consequently reduces H_2O_2 concentrations. To validate this hypothesis, RIR values for NOx were calculated. Although the absolute RIR values for NOx remained negative (-0.06), they were significantly lower than those for NO (-0.9), indicating that the reduction in H_2O_2 due to decreased NO_2 partially offsets the increase in H_2O_2 caused by reduced NO.

Furthermore, the negative RIR value for alkanes (-0.06) suggests that lowering alkane concentrations enhances H_2O_2 production, likely due to their lower photochemical reactivities with OH. When alkane levels are reduced, OH radicals preferentially react with more reactive alkenes and aromatics, leading to increased HO_2 and hence more H_2O_2 formation. The RIR values for alkenes (0.51), aromatics (0.15), and CO (0.26) were consistently positive, indicating that reducing these pollutants is effective in reducing H_2O_2 concentrations, with alkenes exhibiting the most pronounced effect. Consequently, controlling alkenes concentrations within anthropogenic VOCs should be prioritized, aligning with findings from previous studies (Wang et al., 2016; Ye et al., 2021a). Coal combustion and gasoline exhaust were identified as primary sources of alkenes in the region, underscoring the importance of regulating these emissions to mitigate H_2O_2 pollution. Additionally, RIR value for HONO was 0.12, indicating reducing HONO concentrations can further diminish H_2O_2 levels by limiting the primary radical source. Elevated HONO concentrations have been observed across various sites in China, contributing over 40% to primary radical production. Thus, reducing HONO emissions represents a potential mitigating strategy for H_2O_2. Ye et al. (2022) reported that HONO emissions due to fertilizer use significantly increase H_2O_2 levels in rural areas, suggesting that reducing excessive fertilizer use could mitigate H_2O_2 pollution. Moreover, NO_2 heterogeneous reactions at various interfaces and nitrate photolysis are additional sources of HONO (Xue et al., 2020; Xue et al., 2022), highlighting the potential to reduce H_2O_2 by decreasing NO_2 concentrations and subsequently limiting HONO production.

The RIR value for $PM_{2.5}$ (-0.6) was found to be negative, as reducing $PM_{2.5}$ decreases the uptake of H_2O_2, thereby increasing its gas-phase concentration. Recent studies have extensively examined the impact of $PM_{2.5}$ reduction on O_3 concentrations, attributing this phenomenon to diminished HO_2 radical uptake and enhanced photolysis rates, both of which elevate O_3 levels (Wang et al., 2019; Song et al., 2022). These mechanisms similarly contribute to increased H_2O_2 concentrations, yet the effect of particulate matter reduction on H_2O_2 has been largely overlooked. This study demonstrates that $PM_{2.5}$ reduction also decreases H_2O_2 uptake, further exacerbating its gas-phase concentration. This increase in H_2O_2 could enhance sulfate formation efficiency and pose greater threats to human health and ecosystems. Given the critical role of H_2O_2 in atmospheric oxidation capacity, global sulfate aerosol formation, and human health, further research is warranted to investigate H_2O_2 trends, environmental impacts, and mitigation strategies.

3.6 Implications on O_3 formation

H_2O_2 measurements serve as a valuable indicator of O_3 production sensitivity. Under NOx poor conditions, the HO_2 recombination to form H_2O_2 represents the primary radical termination pathway. Conversely, under NOx sufficient conditions, the reaction between NO_2 and OH to form nitric acid (HNO_3) constitutes the dominant termination mechanism. Sillman (1995) identified the H_2O_2/HNO_3 ratio as a robust indicator of O_3 sensitivity, with model simulations revealing that a ratio between 0.2 and 0.3 corresponds to a transitional regime, while values exceeding 0.3 indicate NOx-limited conditions and values below 0.2 suggest VOC-limited conditions. In the absence of direct gaseous HNO_3 measurements, alternative metrics such as H_2O_2/NOy or H_2O_2/NOz can be employed to assess O_3 sensitivity (Sillman et al., 1998), where NOz encompasses HNO_3, PAN, HONO, and alkyl nitrates, and NOy is defined as NOz +NOx.

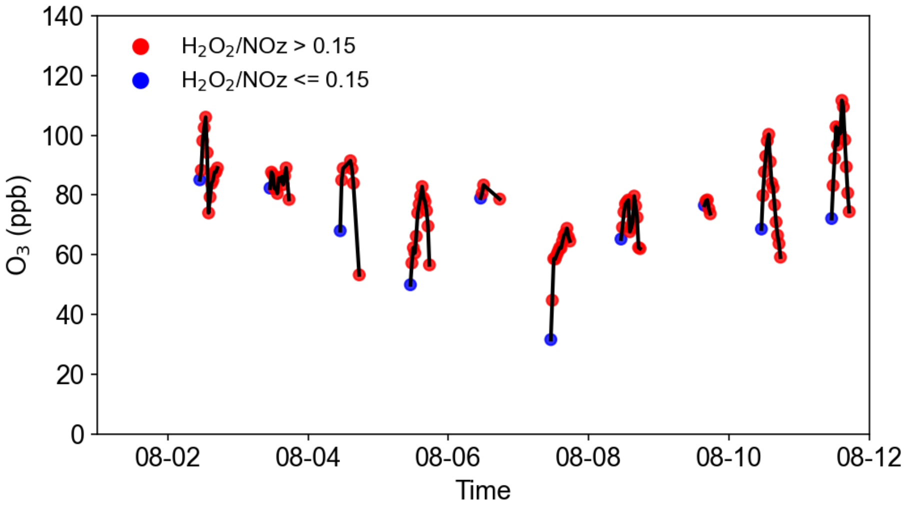

Figure 9. O_3 concentrations values from 1 August to 11 August. The red points represent measurements where H_2O_2/NOz is greater than 0.15, while the blue points correspond to measurements where H_2O_2/NOz is less than or equal to 0.15.

In this study, simultaneous measurements of H_2O_2 and NOz enabled the determination of O_3 sensitivity using the H_2O_2/NOz ratio, with a transitional range identified at 0.15–0.20 (Sillman et al., 1998). The analysis focused on the period of intense photochemical activity between 10:00 and 17:00. As illustrated in Figure 9, over 82% of measured H_2O_2/NOz values exceeded 0.15, indicating that the rural study area predominantly exhibited NOx-limited or transitional conditions during most of the observed period. It is important to note that this metric can be influenced by additional factors. For instance, significant uptake of H_2O_2 by particles was observed in this study, suggesting that the actual photochemical production of H_2O_2 is higher than the measured concentrations. Consequently, the theoretical H_2O_2/NOz ratio is likely greater than the observed values, implying that O_3 production is more strongly aligned with NOx-limited or transitional regimes.

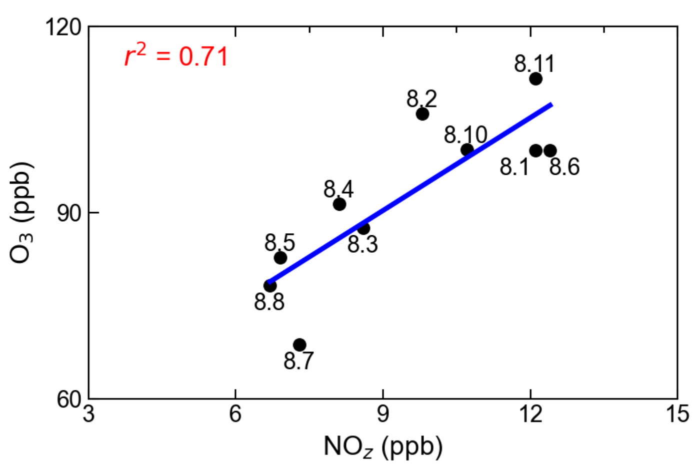

Figure 10. Correlation between daily maxima of O_3 and NOz. The numbers adjacent to the solid dots represent the dates.

To corroborate these findings, the O_3/NOz ratio was also utilized to evaluate O_3 sensitivity. The relationship between peak O_3 concentrations and peak NOz concentrations demonstrated a good positive correlation (r^2=0.71), with a regression slope of 4.98. This slope is comparable with the value (3.3-7.6) reported in a mountainous area north of Beijing (Wang et al., 2006), but lower than those (6-11) observed in Houston (Daum et al., 2004). Notably, the positive correlation persisted up to NOz concentrations of 12 ppb, differing from observations at other sites where the slope typically decreased for NOz levels above 10 ppb (Trainer et al., 1993). This deviation can be attributed to reduced O_3 production efficiency under VOC-limited conditions. However, the sustained positive correlation across the entire study period suggests that the generation of NOz is consistently accompanied by O_3 production, further supporting the prevalence of NOx-sensitive or transitional regimes. These results align with those derived from the H_2O_2/NOz ratio, affirming the utility of H_2O_2/NOz as a reliable indicator of O_3 sensitivity.

The findings underscore the importance of controlling NOx concentrations to mitigate photochemical pollution in rural areas. Tan et al. similarly reported that O_3 production in the rural North China Plain is primarily NOx-limited. As NOx emissions continue to decline due to regulatory efforts, an increasing number of regions may transition into NOx-limited or transitional regimes, highlighting the potential benefits of stringent NOx reduction strategies for future O_3 pollution control. However, given the need for synergistic management of H_2O_2 and O_3, a dual approach targeting both NOx and VOC emissions remains essential. This integrated strategy will be critical for achieving effective and sustainable air quality improvements.

4 Conclusions

To investigate photochemical pollution in rural areas, measurements of H_2O_2 and related parameters were conducted in the Wangdu region during the summer of 2016. H_2O_2 exhibited a distinct diurnal pattern, with an average concentration of 0.62±0.80 ppb. Daily maximum concentrations of H_2O_2 varied significantly, ranging from a minimum of 0.2 ppb to a maximum of 4 ppb. The diurnal cycles of H_2O_2, PAN, and O_3 all followed solar radiation trends, indicating that photochemical reactions predominantly control their production. A good correlation (r^2 = 0.55) was observed between daily maximum concentrations of PAN and O_3, whereas the correlation between maximum concentrations of H_2O_2 and O_3 was weak, suggesting that unidentified processes influencing gas-phase H_2O_2 concentrations may attenuate this relationship. Analysis of the O_3/H_2O_2 ratio revealed that this ratio was significantly higher on polluted days compared to clean days, implying that particle uptake likely reduces gas-phase H_2O_2 concentrations.

To further elucidate the factors influencing H_2O_2 concentrations, a box model was employed. The model simulations initially overestimated H_2O_2 concentrations with a modelled-to-observed ratio of 2.7. However, when H_2O_2 heterogeneous uptake mechanism was incorporated into the model scheme with an uptake coefficient of 6×10^{-4}, the simulated H_2O_2 concentrations aligned well with observed data, underscoring the significant role of heterogeneous uptake in H_2O_2 removal. The primary source of H_2O_2 was identified as the bimolecular recombination of HO_2, contributing 91% of the total source strength, with a maximum production rate of 1 ppb h^{-1}. The dominant removal pathways for H_2O_2 included particle uptake (69%), followed by dry deposition (25%), reaction with OH (4%), and photolysis (2%).

Relative Incremental Reactivity (RIR) analysis demonstrated that reducing NOx, $PM_{2.5}$, and alkanes exacerbated H_2O_2 concentrations, whereas lowering alkenes, aromatics, CO, and HONO effectively reduced H_2O_2 pollution, with alkenes exhibiting the most pronounced impact. The H_2O_2/NOz ratio and the positive correlation between daily peak O_3 and NOz concentrations indicated that O_3 production predominantly occurred in transitional and NOx-limited regimes. To concurrently mitigate H_2O_2 and O_3 pollution, a dual strategy focusing on VOC control and stringent NOx reduction is essential. This approach will be critical for achieving synergistic control of photochemical pollutants in rural areas.

Future research should focus on long-term H_2O_2 monitoring across different environments in the region, refining the parameterization of heterogeneous uptake processes (particularly for HO_2 and H_2O_2 under varying aerosol compositions), and investigating the impacts of changing VOC/NOx ratios on H_2O_2 chemistry. In addition, further research on the interactions between gas-phase oxidants and aerosol processes will be vital for understanding the complex feedback mechanisms that influence air quality in rural and urban environments.

Data availability. The data used in this study are available from the corresponding author upon request (yjmu@rcees.ac.cn).

Author contributions. YM designed the experiments. CY performed H_2O_2 measurements and analyzed the data. CY wrote the manuscript with input from PL and CX. All authors contributed to measurements, discussing results, and commenting on the manuscript.

Competing interests. The contact author has declared that neither they nor their co-authors have any competing interests.

Acknowledgements. We thank the science teams of the summer campaign for their support.

Financial support. This work was supported by the National Natural Science Foundation of China (grant nos. 42305099, 42275111).

References

Allen, H. M., Bates, K. H., Crounse, J. D., Kim, M. J., Teng, A. P., Ray, E. A., and Wennberg, P. O.: H2O2 and CH3OOH (MHP) in the Remote Atmosphere: 2. Physical and Chemical Controls, Journal of Geophysical Research: Atmospheres, 127, e2021JD035702, https://doi.org/10.1029/2021JD035702, 2022.

Ayers, G., Penkett, S., Gillett, R., Bandy, B., Galbally, I., Meyer, C., Elsworth, C., Bentley, S., and Forgan, B.: Evidence for photochemical control of ozone concentrations in unpolluted marine air, Nature, 360, 446-449, 1992.

Balasubramanian, R. and Husain, L.: Observations of gas-phase hydrogen peroxide at an elevated rural site in New York, J Geophys Res-Atmos, 102, 21209-21220, Doi 10.1029/97jd01480, 1997.

Becker, K. H., Brockmann, K. J., and Bechara, J.: Production of hydrogen peroxide in forest air by reaction of ozone with terpenes, Nature, 346, 256-258, 1990.

Calvert, J. G., Lazrus, A., Kok, G. L., Heikes, B. G., Walega, J. G., Lind, J., and Cantrell, C. A.: Chemical Mechanisms of Acid Generation in the Troposphere, Nature, 317, 27-35, Doi 10.1038/317027a0, 1985.

Chen, X., Aoki, M., Takami, A., Chai, F., and Hatakeyama, S.: Effect of ambient-level gas-phase peroxides on foliar injury, growth, and net photosynthesis in Japanese radish (Raphanus sativus), Environ Pollut, 158, 1675-1679, 10.1016/j.envpol.2009.12.002, 2010.

Daum, P. H., Kleinman, L. I., Springston, S. R., Nunnermacker, L. J., Lee, Y. N., Weinstein-Lloyd, J., Zheng, J., and Berkowitz, C. M.: Origin and properties of plumes of high ozone observed during the Texas 2000 Air Quality Study (TexAQS 2000), Journal of Geophysical Research: Atmospheres, 109, https://doi.org/10.1029/2003JD004311, 2004.

de Reus, M., Fischer, H., Sander, R., Gros, V., Kormann, R., Salisbury, G., Van Dingenen, R., Williams, J., Zöllner, M., and Lelieveld, J.: Observations and model calculations of trace gas scavenging in a dense Saharan dust plume during MINATROC, Atmos. Chem. Phys., 5, 1787-1803, 10.5194/acp-5-1787-2005, 2005.

Fischer, H., Pozzer, A., Schmitt, T., Jöckel, P., Klippel, T., Taraborrelli, D., and Lelieveld, J.: Hydrogen peroxide in the marine boundary layer over the South Atlantic during the OOMPH cruise in March 2007, Atmos Chem Phys, 15, 6971-6980, 2015.

Fischer, H., Axinte, R., Bozem, H., Crowley, J. N., Ernest, C., Gilge, S., Hafermann, S., Harder, H., Hens, K., and Janssen, R. H.: Diurnal variability, photochemical production and loss processes of hydrogen peroxide in the boundary layer over Europe, Atmos Chem Phys, 19, 11953-11968, 2019.

Gao, J., Wang, H., Liu, W., Xu, H., Wei, Y., Tian, X., Feng, Y., Song, S., and Shi, G.: Hydrogen peroxide serves as pivotal fountainhead for aerosol aqueous sulfate formation from a global perspective, Nat Commun, 15, 4625, 10.1038/s41467-024-48793-1, 2024.

George, I. J., Matthews, P. S. J., Whalley, L. K., Brooks, B., Goddard, A., Baeza-Romero, M. T., and Heard, D. E.: Measurements of uptake coefficients for heterogeneous loss of HO2 onto submicron inorganic salt aerosols, Phys Chem Chem Phys, 15, 12829-12845, 10.1039/C3CP51831K, 2013.

Guo, J., Wang, Z., Cui, Y., and Zhang, X.: Assessment of the H2O2 budget at an urban site concerning the HO2 underprediction and the vertical transport from residual layers, Atmos Environ, 272, 118952, https://doi.org/10.1016/j.atmosenv.2022.118952, 2022.

Guo, J., Tilgner, A., Yeung, C., Wang, Z., Louie, P. K. K., Luk, C. W. Y., Xu, Z., Yuan, C., Gao, Y., Poon, S., Herrmann, H., Lee, S., Lam, K. S., and Wang, T.: Atmospheric Peroxides in a Polluted Subtropical Environment: Seasonal Variation, Sources and Sinks, and Importance of Heterogeneous Processes, Environ Sci Technol, 48, 1443-1450, 10.1021/es403229x, 2014.

He, S. Z., Chen, Z. M., Zhang, X., Zhao, Y., Huang, D. M., Zhao, J. N., Zhu, T., Hu, M., and Zeng, L. M.: Measurement of atmospheric hydrogen peroxide and organic peroxides in Beijing before and during the 2008 Olympic Games: Chemical and physical factors influencing their concentrations, J Geophys Res-Atmos, 115, Artn D17307
10.1029/2009jd013544, 2010.

Hua, W., Chen, Z. M., Jie, C. Y., Kondo, Y., Hofzumahaus, A., Takegawa, N., Chang, C. C., Lu, K. D., Miyazaki, Y., Kita, K., Wang, H. L., Zhang, Y. H., and Hu, M.: Atmospheric hydrogen peroxide and organic hydroperoxides during PRIDE-

PRD'06, China: their concentration, formation mechanism and contribution to secondary aerosols, Atmos Chem Phys, 8, 6755-6773, DOI 10.5194/acp-8-6755-2008, 2008.

Kanaya, Y., Cao, R., Akimoto, H., Fukuda, M., Komazaki, Y., Yokouchi, Y., Koike, M., Tanimoto, H., Takegawa, N., and Kondo, Y.: Urban photochemistry in central Tokyo: 1. Observed and modeled OH and HO2 radical concentrations during the winter and summer of 2004, Journal of Geophysical Research: Atmospheres, 112, https://doi.org/10.1029/2007JD008670, 2007a.

Kanaya, Y., Tanimoto, H., Matsumoto, J., Furutani, H., Hashimoto, S., Komazaki, Y., Tanaka, S., Yokouchi, Y., Kato, S., Kajii, Y., and Akimoto, H.: Diurnal variations in H2O2, O3, PAN, HNO3 and aldehyde concentrations and NO/NO2 ratios at Rishiri Island, Japan: Potential influence from iodine chemistry, Sci Total Environ, 376, 185-197, https://doi.org/10.1016/j.scitotenv.2007.01.073, 2007b.

Klippel, T., Fischer, H., Bozem, H., Lawrence, M. G., Butler, T., Jöckel, P., Tost, H., Martinez, M., Harder, H., and Regelin, E.: Distribution of hydrogen peroxide, methyl hydroperoxide and formaldehyde over central Europe during the HOOVER project, Atmos Chem Phys, 11, 4391-4410, 2011.

Lakey, P. S. J., George, I. J., Whalley, L. K., Baeza-Romero, M. T., and Heard, D. E.: Measurements of the HO2 Uptake Coefficients onto Single Component Organic Aerosols, Environ Sci Technol, 49, 4878-4885, 10.1021/acs.est.5b00948, 2015.

Lazrus, A. L., Kok, G. L., Lind, J. A., Gitlin, S. N., Heikes, B. G., and Shetter, R. E.: Automated Fluorometric Method for Hydrogen-Peroxide in Air, Anal Chem, 58, 594-597, Doi 10.1021/Ac00294a024, 1986.

Lee, G., Jang, Y., Lee, H., Han, J.-S., Kim, K.-R., and Lee, M.: Characteristic behavior of peroxyacetyl nitrate (PAN) in Seoul megacity, Korea, Chemosphere, 73, 619-628, https://doi.org/10.1016/j.chemosphere.2008.05.060, 2008a.

Lee, M., Kie, J. A., Kim, Y. M., and Lee, G.: Characteristics of atmospheric hydrogen peroxide variations in Seoul megacity during 2002-2004, Sci Total Environ, 393, 299-308, 10.1016/j.scitotenv.2007.11.037, 2008b.

Li, J. R., Zhu, C., Chen, H., Fu, H. B., Xiao, H., Wang, X. F., Herrmann, H., and Chen, J. M.: A More Important Role for the Ozone-S(IV) Oxidation Pathway Due to Decreasing Acidity in Clouds, J Geophys Res-Atmos, 125, 2020.

Li, K., Jacob, D. J., Liao, H., Shen, L., Zhang, Q., and Bates, K. H.: Anthropogenic drivers of 2013-2017 trends in summer surface ozone in China, P Natl Acad Sci USA, 116, 422-427, 10.1073/pnas.1812168116, 2019.

Liang, H., Chen, Z. M., Huang, D., Zhao, Y., and Li, Z. Y.: Impacts of aerosols on the chemistry of atmospheric trace gases: a case study of peroxides and HO2 radicals, Atmos Chem Phys, 13, 11259-11276, 10.5194/acp-13-11259-2013, 2013.

Liu, P., Ye, C., Zhang, C., He, G., Xue, C., Liu, J., Liu, C., Zhang, Y., Song, Y., Li, X., Wang, X., Chen, J., He, H., Herrmann, H., and Mu, Y.: Photochemical Aging of Atmospheric Fine Particles as a Potential Source for Gas-Phase Hydrogen Peroxide, Environ Sci Technol, 55, 15063-15071, 10.1021/acs.est.1c04453, 2021.

Liu, Y., Geng, G., Cheng, J., Liu, Y., Xiao, Q., Liu, L., Shi, Q., Tong, D., He, K., and Zhang, Q.: Drivers of Increasing Ozone during the Two Phases of Clean Air Actions in China 2013–2020, Environ Sci Technol, 57, 8954-8964, 10.1021/acs.est.3c00054, 2023.

Lu, X., Zhang, L., Wang, X., Gao, M., Li, K., Zhang, Y., Yue, X., and Zhang, Y.: Rapid Increases in Warm-Season Surface Ozone and Resulting Health Impact in China Since 2013, Environmental Science & Technology Letters, 7, 240-247, 2020.

Ma, X., Tan, Z., Lu, K., Yang, X., Chen, X., Wang, H., Chen, S., Fang, X., Li, S., Li, X., Liu, J., Liu, Y., Lou, S., Qiu, W., Wang, H., Zeng, L., and Zhang, Y.: OH and HO_2 radical chemistry at a suburban site during the EXPLORE-YRD campaign in 2018, Atmos. Chem. Phys., 22, 7005-7028, 10.5194/acp-22-7005-2022, 2022.

Ma, Z., Xu, J., Quan, W., Zhang, Z., Lin, W., and Xu, X.: Significant increase of surface ozone at a rural site, north of eastern China, Atmos. Chem. Phys., 16, 3969-3977, 10.5194/acp-16-3969-2016, 2016.

Nunnermacker, L. J., Weinstein-Lloyd, J. B., Hillery, B., Giebel, B., Kleinman, L. I., Springston, S. R., Daum, P. H., Gaffney, J., Marley, N., and Huey, G.: Aircraft and ground-based measurements of hydroperoxides during the 2006 MILAGRO field campaign, Atmos Chem Phys, 8, 7619-7636, 10.5194/acp-8-7619-2008, 2008.

Peng, X., Wang, W., Xia, M., Chen, H., Ravishankara, A. R., Li, Q., Saiz-Lopez, A., Liu, P., Zhang, F., Zhang, C., Xue, L., Wang, X., George, C., Wang, J., Mu, Y., Chen, J., and Wang, T.: An unexpected large continental source of reactive bromine and chlorine with significant impact on wintertime air quality, National Science Review, 8, nwaa304, 10.1093/nsr/nwaa304, 2021.

Penkett, S. A., Jones, B. M. R., Brice, K. A., and Eggleton, A. E. J.: Importance of Atmospheric Ozone and Hydrogen-Peroxide in Oxidizing Sulfur-Dioxide in Cloud and Rainwater, Atmos Environ, 13, 123-137, Doi 10.1016/0004-6981(79)90251-8, 1979.

Pradhan, M., Kalberer, M., Griffiths, P. T., Braban, C. F., Pope, F. D., Cox, R. A., and Lambert, R. M.: Uptake of Gaseous Hydrogen Peroxide by Submicrometer Titanium Dioxide Aerosol as a Function of Relative Humidity, Environ Sci Technol, 44, 1360-1365, 10.1021/es902916f, 2010.

Qin, M., Chen, Z., Shen, H., Li, H., Wu, H., and Wang, Y.: Impacts of heterogeneous reactions to atmospheric peroxides: Observations and budget analysis study, Atmos Environ, 183, 144-153, 10.1016/j.atmosenv.2018.04.005, 2018.

Qin, X., Chen, Z., Gong, Y., Dong, P., Cao, Z., Hu, J., and Xu, J.: Persistent Uptake of H_2O_2 onto Ambient $PM_{2.5}$ via Dark-Fenton Chemistry, Environ Sci Technol, 56, 9978-9987, 10.1021/acs.est.2c03630, 2022.

Rao, Z., Fang, Y.-G., Pan, Y., Yu, W., Chen, B., Francisco, J. S., Zhu, C., and Chu, C.: Accelerated Photolysis of H_2O_2 at the Air–Water Interface of a Microdroplet, Journal of the American Chemical Society, 145, 24717-24723, 10.1021/jacs.3c08101, 2023.

Reeves, C. E. and Penkett, S. A.: Measurements of peroxides and what they tell us, Chem Rev, 103, 5199-5218, 10.1021/cr0205053, 2003.

Ren, Y., Ding, A. J., Wang, T., Shen, X. H., Guo, J., Zhang, J. M., Wang, Y., Xu, P. J., Wang, X. F., Gao, J., and Collett, J. L.: Measurement of gas-phase total peroxides at the summit of Mount Tai in China, Atmos Environ, 43, 1702-1711, 10.1016/j.atmosenv.2008.12.020, 2009.

Romanias, M. N., El Zein, A., and Bedjanian, Y.: Heterogeneous Interaction of H_2O_2 with TiO_2 Surface under Dark and UV Light Irradiation Conditions, The Journal of Physical Chemistry A, 116, 8191-8200, 10.1021/jp305366v, 2012.

Sillman, S.: The use of NO_y, H_2O_2, and HNO_3 as indicators for ozone-NO_x-hydrocarbon sensitivity in urban locations, Journal of Geophysical Research: Atmospheres, 100, 14175-14188, 1995.

Sillman, S., He, D., Pippin, M. R., Daum, P. H., Imre, D. G., Kleinman, L. I., Lee, J. H., and Weinstein-Lloyd, J.: Model correlations for ozone, reactive nitrogen, and peroxides for Nashville in comparison with measurements: Implications for O_3-NO_x-hydrocarbon chemistry, Journal of Geophysical Research: Atmospheres, 103, 22629-22644, 1998.

Sofen, E. D., Alexander, B., and Kunasek, S. A.: The impact of anthropogenic emissions on atmospheric sulfate production pathways, oxidants, and ice core $\Delta O^{17}(SO_4^{2-})$, Atmos. Chem. Phys., 11, 3565-3578, 10.5194/acp-11-3565-2011, 2011.

Song, H., Lu, K., Dong, H., Tan, Z., Chen, S., Zeng, L., and Zhang, Y.: Reduced Aerosol Uptake of Hydroperoxyl Radical May Increase the Sensitivity of Ozone Production to Volatile Organic Compounds, Environmental Science & Technology Letters, 9, 22-29, 10.1021/acs.estlett.1c00893, 2022.

Sun, M., Cui, J. n., Zhao, X., and Zhang, J.: Impacts of precursors on peroxyacetyl nitrate (PAN) and relative formation of PAN to ozone in a southwestern megacity of China, Atmos Environ, 231, 117542, https://doi.org/10.1016/j.atmosenv.2020.117542, 2020.

Takami, A., Shiratori, N., Yonekura, H., and Hatakeyama, S.: Measurement of hydroperoxides and ozone in Oku-Nikko area, Atmos Environ, 37, 3861-3872, 10.1016/S1352-2310(03)00454-0, 2003.

Taketani, F., Kanaya, Y., Pochanart, P., Liu, Y., Li, J., Okuzawa, K., Kawamura, K., Wang, Z., and Akimoto, H.: Measurement of overall uptake coefficients for HO2 radicals by aerosol particles sampled from ambient air at Mts. Tai and Mang (China), Atmos. Chem. Phys., 12, 11907-11916, 10.5194/acp-12-11907-2012, 2012.

Tan, Z., Hofzumahaus, A., Lu, K., Brown, S. S., Holland, F., Huey, L. G., Kiendler-Scharr, A., Li, X., Liu, X., Ma, N., Min, K.-E., Rohrer, F., Shao, M., Wahner, A., Wang, Y., Wiedensohler, A., Wu, Y., Wu, Z., Zeng, L., Zhang, Y., and Fuchs, H.: No Evidence for a Significant Impact of Heterogeneous Chemistry on Radical Concentrations in the North China Plain in Summer 2014, Environ Sci Technol, 54, 5973-5979, 10.1021/acs.est.0c00525, 2020.

Tan, Z., Fuchs, H., Lu, K., Hofzumahaus, A., Bohn, B., Broch, S., Dong, H., Gomm, S., Häseler, R., He, L., Holland, F., Li, X., Liu, Y., Lu, S., Rohrer, F., Shao, M., Wang, B., Wang, M., Wu, Y., Zeng, L., Zhang, Y., Wahner, A., and Zhang, Y.: Radical chemistry at a rural site (Wangdu) in the North China Plain: observation and model calculations of OH, HO2 and RO2 radicals, Atmos. Chem. Phys., 17, 663-690, 10.5194/acp-17-663-2017, 2017.

Tang, M. J., Huang, X., Lu, K. D., Ge, M. F., Li, Y. J., Cheng, P., Zhu, T., Ding, A. J., Zhang, Y. H., Gligorovski, S., Song, W., Ding, X., Bi, X. H., and Wang, X. M.: Heterogeneous reactions of mineral dust aerosol: implications for tropospheric oxidation capacity, Atmos Chem Phys, 17, 11727-11777, 10.5194/acp-17-11727-2017, 2017.

Thornton, J. A., Jaeglé, L., and McNeill, V. F.: Assessing known pathways for HO2 loss in aqueous atmospheric aerosols: Regional and global impacts on tropospheric oxidants, Journal of Geophysical Research: Atmospheres, 113, https://doi.org/10.1029/2007JD009236, 2008.

Trainer, M., Parrish, D. D., Buhr, M. P., Norton, R. B., Fehsenfeld, F. C., Anlauf, K. G., Bottenheim, J. W., Tang, Y. Z., Wiebe, H. A., Roberts, J. M., Tanner, R. L., Newman, L., Bowersox, V. C., Meagher, J. F., Olszyna, K. J., Rodgers, M. O., Wang, T., Berresheim, H., Demerjian, K. L., and Roychowdhury, U. K.: Correlation of ozone with NOy in photochemically aged air, Journal of Geophysical Research: Atmospheres, 98, 2917-2925, https://doi.org/10.1029/92JD01910, 1993.

Walker, S. J., Evans, M. J., Jackson, A. V., Steinbacher, M., Zellweger, C., and McQuaid, J. B.: Processes controlling the concentration of hydroperoxides at Jungfraujoch Observatory, Switzerland, Atmos Chem Phys, 6, 5525-5536, DOI 10.5194/acp-6-5525-2006, 2006.

Wang, T., Ding, A., Gao, J., and Wu, W. S.: Strong ozone production in urban plumes from Beijing, China, Geophys Res Lett, 33, 2006.

Wang, W., Li, X., Shao, M., Hu, M., Zeng, L., Wu, Y., and Tan, T.: The impact of aerosols on photolysis frequencies and ozone production in Beijing during the 4-year period 2012–2015, Atmos. Chem. Phys., 19, 9413-9429, 10.5194/acp-19-9413-2019, 2019.

Wang, W., Parrish, D. D., Li, X., Shao, M., Liu, Y., Mo, Z., Lu, S., Hu, M., Fang, X., Wu, Y., Zeng, L., and Zhang, Y.: Exploring the drivers of the increased ozone production in Beijing in summertime during 2005–2016, Atmos. Chem. Phys., 20, 15617-15633, 10.5194/acp-20-15617-2020, 2020.

Wang, Y., Chen, Z. M., Wu, Q. Q., Liang, H., Huang, L. B., Li, H., Lu, K. D., Wu, Y. S., Dong, H. B., Zeng, L. M., and Zhang, Y. H.: Observation of atmospheric peroxides duringWangdu Campaign 2014 at a rural site in the North China Plain, Atmos Chem Phys, 16, 10985-11000, 10.5194/acp-16-10985-2016, 2016.

Watanabe, K., Yachi, C., Nishibe, M., Michigami, S., Saito, Y., Eda, N., Yamazaki, N., and Hirai, T.: Measurements of atmospheric hydroperoxides over a rural site in central Japan during summers using a helicopter, Atmos Environ, 146, 174-182, 2016.

Watkins, B. A., Parrish, D. D., Buhr, S., Norton, R. B., Trainer, M., Yee, J. E., and Fehsenfeld, F. C.: Factors influencing the concentration of gas phase hydrogen peroxide during the summer at Kinterbish, Alabama, Journal of Geophysical Research: Atmospheres, 100, 22841-22851, https://doi.org/10.1029/95JD01533, 1995.

Whalley, L. K., Furneaux, K. L., Goddard, A., Lee, J. D., Mahajan, A., Oetjen, H., Read, K. A., Kaaden, N., Carpenter, L. J., Lewis, A. C., Plane, J. M. C., Saltzman, E. S., Wiedensohler, A., and Heard, D. E.: The chemistry of OH and HO2 radicals in the boundary layer over the tropical Atlantic Ocean, Atmos. Chem. Phys., 10, 1555-1576, 10.5194/acp-10-1555-2010, 2010.

Xu, W., Zhang, G., Wang, Y., Tong, S., Zhang, W., Ma, Z., Lin, W., Kuang, Y., Yin, L., and Xu, X.: Aerosol Promotes Peroxyacetyl Nitrate Formation During Winter in the North China Plain, Environ Sci Technol, 55, 3568-3581, 10.1021/acs.est.0c08157, 2021.

Xue, C., Ye, C., Kleffmann, J., Zhang, W., He, X., Liu, P., Zhang, C., Zhao, X., Liu, C., Ma, Z., Liu, J., Wang, J., Lu, K., Catoire, V., Mellouki, A., and Mu, Y.: Atmospheric measurements at Mt. Tai – Part II: HONO budget and radical (ROx+NO3) chemistry in the lower boundary layer, Atmos. Chem. Phys., 22, 1035-1057, 10.5194/acp-22-1035-2022, 2022.

Xue, C. Y., Zhang, C. L., Ye, C., Liu, P. F., Catoire, V., Krysztofiak, G., Chen, H., Ren, Y. G., Zhao, X. X., Wang, J. H., Zhang, F., Zhang, C. X., Zhang, J. W., An, J. L., Wang, T., Chen, J. M., Kleffmann, J., Mellouki, A., and Mu, Y. J.: HONO Budget and Its Role in Nitrate Formation in the Rural North China Plain, Environ Sci Technol, 54, 11048-11057, 2020.

Ye, C., Liu, P., Ma, Z., Xue, C., Zhang, C., Zhang, Y., Liu, J., Liu, C., Sun, X., and Mu, Y.: High H2O2 Concentrations Observed during Haze Periods during the Winter in Beijing: Importance of H2O2 Oxidation in Sulfate Formation, Environmental Science & Technology Letters, 10.1021/acs.estlett.8b00579, 2018.

Ye, C., Xue, C., Liu, P., Zhang, C., Ma, Z., Zhang, Y., Liu, C., Liu, J., Lu, K., and Mu, Y.: Strong impacts of biomass burning, nitrogen fertilization, and fine particles on gas-phase hydrogen peroxide (H2O2), Sci Total Environ, 843, 156997, https://doi.org/10.1016/j.scitotenv.2022.156997, 2022.

Ye, C., Xue, C., Zhang, C., Ma, Z., Liu, P., Zhang, Y., Liu, C., Zhao, X., Zhang, W., He, X., Song, Y., Liu, J., Wang, W., Sui, B., Cui, R., Yang, X., Mei, R., Chen, J., and Mu, Y.: Atmospheric Hydrogen Peroxide (H2O2) at the Foot and Summit of Mt. Tai: Variations, Sources and Sinks, and Implications for Ozone Formation Chemistry, Journal of Geophysical Research: Atmospheres, 126, e2020JD033975, https://doi.org/10.1029/2020JD033975, 2021a.

Ye, C., Chen, H., Hoffmann, E. H., Mettke, P., Tilgner, A., He, L., Mutzel, A., Brüggemann, M., Poulain, L., Schaefer, T., Heinold, B., Ma, Z., Liu, P., Xue, C., Zhao, X., Zhang, C., Zhang, F., Sun, H., Li, Q., Wang, L., Yang, X., Wang, J., Liu, C., Xing, C., Mu, Y., Chen, J., and Herrmann, H.: Particle-Phase Photoreactions of HULIS and TMIs Establish a Strong Source of H2O2 and Particulate Sulfate in the Winter North China Plain, Environ Sci Technol, 55, 7818-7830, 10.1021/acs.est.1c00561, 2021b.

Zhang, G., Mu, Y. J., Liu, J. F., Zhang, C. L., Zhang, Y. Y., Zhang, Y. J., and Zhang, H. X.: Seasonal and diurnal variations of atmospheric peroxyacetyl nitrate, peroxypropionyl nitrate, and carbon tetrachloride in Beijing, J Environ Sci-China, 26, 65-74, 10.1016/S1001-0742(13)60382-4, 2014.

Zhang, Q., Liu, J., He, Y., Yang, J., Gao, J., Liu, H., Tang, W., Chen, Y., Fan, W., Chen, X., Chai, F., and Hatakeyama, S.: Measurement of hydrogen peroxide and organic hydroperoxide concentrations during autumn in Beijing, China, J Environ Sci-China, 64, 72-81, https://doi.org/10.1016/j.jes.2016.12.015, 2018.

Zhang, X., He, S. Z., Chen, Z. M., Zhao, Y., and Hua, W.: Methyl hydroperoxide (CH3OOH) in urban, suburban and rural atmosphere: ambient concentration, budget, and contribution to the atmospheric oxidizing capacity, Atmos. Chem. Phys., 12, 8951-8962, 10.5194/acp-12-8951-2012, 2012.